

Synchronous Reluctance Machines: A Comprehensive Review and Technology Comparison

¹Mukhammed Murataliyev, *Member, IEEE*, Michele Degano, *Senior Member, IEEE*, Mauro Di Nardo, *Member IEEE*, Nicola Bianchi, *Fellow Member, IEEE*, Chris Gerada, *Senior Member, IEEE*

Abstract— In the last decade, the trend towards higher efficiency and higher torque density electrical machines without permanent magnets for industrial sector has rapidly increased. This work discusses the latest research and industrial advancements in Synchronous Reluctance machines (SynRM), being the emergent motor topology gaining wide acceptance by many industries. The paper presents an extensive literature review covering the background and evolution of SynRM, including the most recent developments. Nowadays, SynRM has found its niche in the electrical machines market, and the reasons for that are highlighted in this work together with its advantages and disadvantages. The key journal publications in SynRM topics are discussed presenting the biggest challenges and latest advancements with particular regards to the design methodology. This paper aims to provide a thorough overview to the research community and industry about SynRM. There is a clear potential for SynRM to take over significant portion of electrical machine market in the near future to meet efficiency standards in industrial applications without the use of rare-earth permanent magnet technology.

Index Terms— Synchronous Reluctance Machines, Review, Industrial Drives, Design Methods, High efficiency.

I. INTRODUCTION

In recent years, there is a growing interest for high efficiency electric motors without, or with reduced content of permanent magnets (PMs). SynRM is one of the most promising candidates that can meet these requirements along with the high efficiency and low cost [1], [2]. The root of all its benefits and drawbacks are related to its rotor structure. The latter is made of a suitably cut stack of laminations without using any excitation coils as in wound rotor machines, short-circuited conductors as in Squirrel Cage IMs (SCIM) or PMs in PM machines [3]. This leads to a cost-effective structure that is using the reluctance principle to generate torque.

The SynRM topology was first introduced in 1920s [4], however it was not applicable to industrial applications as other technologies such as SCIMs as this can be directly fed from 3-phase supply [5]. SCIMs are still considered the industry “work horse” as it dominates the electrical machines (EM) market in applications such as industrial fans, pumps, and mill type loads. Indeed, it is the cheapest and the most reliable machine

topology based on mature manufacturing processes. In the 60s’, after a few decades of research, PMs started to be used for applications requiring high performance.

The rare-earth permanent magnets started to be commercialized for electrical motors in early 1980s, introducing a new revolution for the EM sector, thanks to their high energy density, with respect to previous hard magnetic materials. Various types of applications such as high-performance industrial motors for spindles and compressors, Electric Vehicles (EV), wind turbines, actuators, started to adopt PM synchronous machines [6], [7], [8]. Neodymium-iron-boron (NdFeB) PMs are the most common type of magnets for high-performance applications due to their superior magnetic properties. In comparison, the remanent flux density B_r and coercivity H_c values of NdFeB are higher than any other type of magnets such as Samarium-Cobalt (Sm2Co17), which was the major breakthrough in 1970s [9], and it is still extensively used when high operating temperatures are required.

The main downfall of NdFeB magnets is their cost moreover their future availability and embedded carbon emission in their manufacturing processes are also concerning issues. The prices of the PM saw a huge spike in the mid-2011, as it increased by factor of 25 compared to the beginning of 2010 [10], [11]. After hitting its peak, the price dropped rapidly and settled at its pre-bubble price [12]. Such price instability had a huge financial effect on PM machine manufacturers. Hence, in the following years the research on EMs with low usage of rare earth-based PMs was intensified [13], [14].

Along with this cost and supply chain concerns, industrial applications have to comply with various standards and regulations, all tending to increase the minimum energy efficiency [3], [15], [16]. This was driven by national and international policies aimed at improving the way energy is produced and consumed, and so minimize the human footprint and the related greenhouse gas emissions [17], [18].

Currently world leading manufacturers and R&D institutions are constantly investigating the possibility of increasing the efficiency using cost-effective solutions. SynRM is a promising technology with features that are well aligned with the above industrial needs: high efficiency and no-magnets [10], [12].

¹ Manuscript received April 18, 2021; revised October 6, 2021, accepted January 18, 2022.

M. Murataliyev, M. Degano, M. Di Nardo and C. Gerada are with the PEMC Group, University of Nottingham, Nottingham, UK., (email:

m.murataliyev@nottingham.ac.uk michele.degano@nottingham.ac.uk , mauro.dinardo4@nottingham.ac.uk chris.gerada@nottingham.ac.uk)

Nicola Bianchi is with the Department of Electrical Engineering, University of Padova, Italy (email: nicola.bianchi@unipd.it)

Key EM manufacturers such as ABB, KSB and Siemens have already started the serial production of the high efficiency SynRM [19], [20]. In addition to this, there is a great potential for SynRM in automotive applications as these also requires extended field weakening capabilities which can be achieved using low energy density PM.

Despite its advantages, there are still number of issues that are subject of research. From the machine design perspective, the main challenges come from the complex anisotropic structure of the rotor requiring a non-standard design procedure. Torque ripple, power factor (PF) and other secondary effects such as rotor iron losses, vibration, and noise, are the main issues that need to be carefully considered during the design of a SynRM [21], [22].

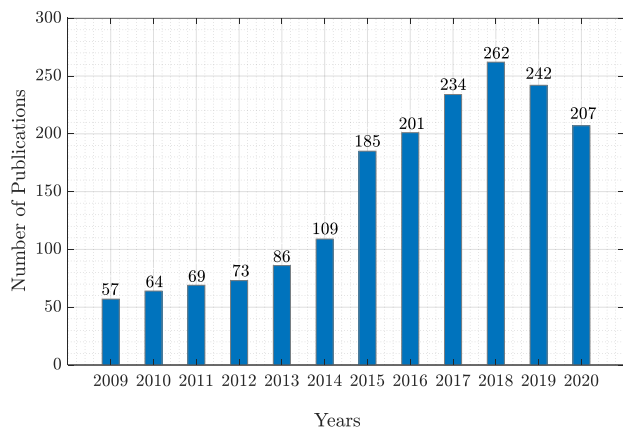


Fig. 1. Number of Publications on SynRM topic over the past decade. [1]

According to statistics that were acquired via Google Scholar, from 2009 to late 2020, IEEE, IET, Elsevier have published 1789 scientific papers on SynRM meanwhile PM motors technologies had over 12000 manuscripts. Fig. 1 presents the number of publications on SynRM topic over the past decade. As can be observed, the scientific interest towards SynRM has been constantly growing due to current trends

towards rare earth element (REE) free technologies and more energy efficient EMs.

This paper covers the main reasons why SynRM is gaining the industry’s attention as well as the recent developments of this topology.

Chapter II is dedicated to efficiency roadmaps and aims to cover recent and future government regulations for higher efficiency drives. Chapter III discusses the main economical as well as the supply chain problems of the REE PMs. Basic operational principles of the SynRM in the context of other synchronous EM topologies are discussed in Chapter IV. In Chapter V the state of the art of is reported. It discusses main design challenges as well as the drawbacks of the SynRM, and design methods to address them. Modern design ideas and innovative techniques introduced by the research community with the aim of significantly reducing the effort required to design SynRM are all discussed in detail. Chapter VI is dedicated to a discussion of SynRM as a potential modern industrial EM. A detailed comparison of the SynRM with other widely spread industrial topologies such as SCIM and PM machines is reported. Different SynRM application examples are discussed including an example of a Line-Start SynRM. A detailed qualitative cost comparison of SynRM with SCIM is presented. Finally, in Chapter VII, paper provides examples of industrial SynRM that is currently available on the market, to prove the wide acceptance of SynRM by the industry.

II. New EM Efficiency Roadmaps

As reported in [23], [24] electrical machines consume approximately 40% of the total worldwide generated electrical energy, whereas in EU EMs take almost 70% of the total consumed electrical energy. Therefore, improvements in the EM energy efficiency could lead to significant reduction in power consumption and related carbon emission. The main EU energy and climate goal of the 2020 is to achieve the reduction in the greenhouse gas emissions by 20% compared to the 1990 levels [25], [26], by raising the share of the power generation

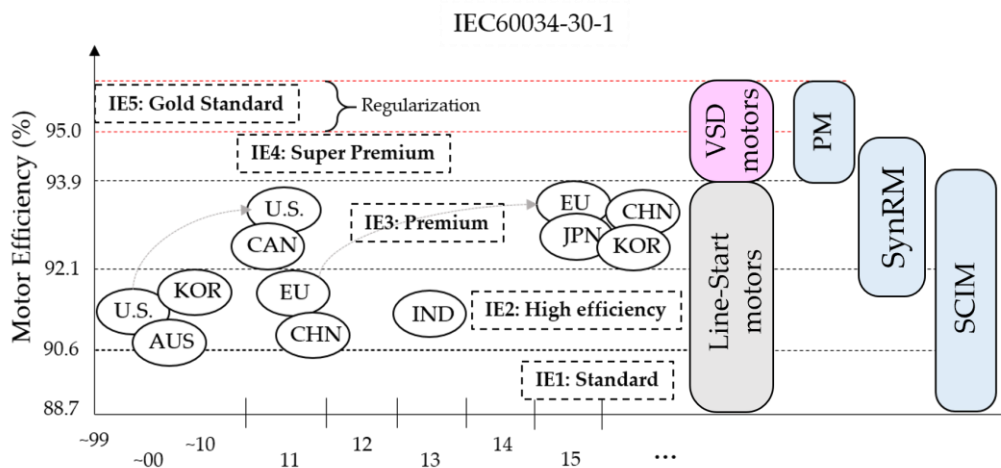


Fig. 2. Electrical Machines Efficiency movement timeline, standard 15kW motor example. [39]

from renewable resources. New regulations according to the 2030 Framework on Climate and Energy were set in 2014 by the European Commission on January 22nd and by European Council on October 24th. The next milestone was set for a mandatory 40% reduction in greenhouse gas emissions from the 1990 levels and 27% of the total generated power should come from the renewable sources, with a target of 27% in terms of energy savings to be achieved.

According to [27], 56% of the motors worldwide exceeds their life expectancy. 68% of the utilized motors are oversized having the load that is less by 60% or sometimes 80% of their rated capability. The older machines (normally used to drive fans, pumps, compressors, etc.) are inefficient and usually fall under IE0/IE1 standards. Moreover, they are less reliable and less performing and require constant maintenance and repair. One of the biggest worldwide industrial problems is the lack of a machine renewal culture [27].

It was highlighted in [28], that the acceptance of the higher efficiency standards for EMs is affected by the existence of the common standards of the motor performance tests, efficiency classification and labelling. The IE4 Standard was introduced in the 1st edition of the IEC 60034-30, whereas the Gold Standard Efficiency IE5 was introduced in the 2nd edition.

Three phase SCIM take a major portion of the EM market [12], [10]. Currently major manufacturers already have the capability to produce the SCIMs that meet the IE4 class, by using standard frames with aluminum rotor cages [29], [30]. Line start PM machine (LSPM) is another IE4 class motor, usually it has the interior rare earth PMs (NdFeB) and auxiliary cage for starting.

Fig. 2 shows the motor efficiency classes adoption timeline in different countries (15kW drive example). Fig. 2 was retrieved from [31], however it was modified by adding SynRM efficiency capability based on [32], [19]. The standards highlighted in Fig. 2 are applicable for EMs within a power range between 120W and 1000kW with voltages up to 6kV, number of poles of considered machines are 2 to 8, whereas the thermal operating conditions are between -20°C up to 60°C at 4000m altitude [33]. Based on the efficiency trends and the capability of SCIMs and PM machine topologies, it can be stated that SynRM can surely have a significant role within the IE4 Premium Efficiency band.

A. Efficiency standard timeline

The strong push towards high efficiency is dictated by the recent EU environmental policies. These are reported in [28], [34], [35]. The Eco-Design directive is divided into several policy options (PO), listed as follow:

- PO-1 was accepted on 1st January 2018 and includes:
 - PO-1A which targets all single phase motors rated above 0.12kW imposing at least the IE2 standard;
 - PO-1B implies that three phase motors with rated power greater than 120W and less than 750W should meet the IE2 standard or greater;

- PO-1C involves that all three phase low voltage (LV) and medium voltage (MV) motors rated above 375kW and below 1000kW should meet IE3 standard or greater
- PO-2 should be accepted by 1st January 2022 and implies that all the VSDs rated above 750W should meet IE3 standard;
- PO-3 was accepted on 1st January 2018 and included the explosion proof, brake motors and other Ex-eb² motors;
- PO-4 was accepted on 1st January 2018 and included mandatory requirements for motors and VSD (discussed later);
- PO-5 was accepted on 1st January 2018 and imposed that all VSDs meet the IE1 performance at minimum energy performance standards (MEPS);
- PO-6 should be accepted by 1st January 2022 and includes:
 - PO-6A where MEPS should be raised for SCIMs greater than 750W and less than 375kW from IE3 to IE4;
 - PO-6B where MEPS of larger SCIMs (between 375kW and 1MW) should go from IE3 to IE4.

PO4 states that all machine product information requirements as well as the comprehensive detailed technical information should be included on the rating plate for all motors that are rated 120W – 1MW. The PO5 was introduced to eliminate the usage of the VSD motors that are below IE1 standard. PO-6 mainly focuses on the transition to IE4 that should be available at the competitive prices compared to IE3 machines.

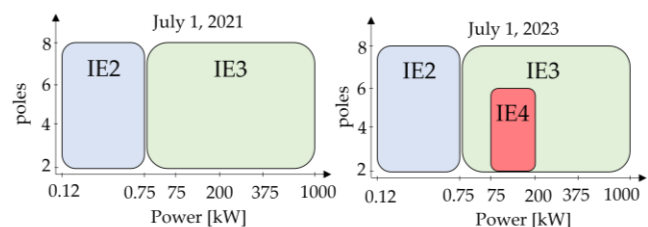


Fig. 3. Efficiency regulations 2021-2023.

B. Recent efficiency regulations

A very recent efficiency requirement (PO-6A) that took effect on July 1st, 2021 states that all motors with rated output power greater than 750W and less than 1000kW with 2, 4, 6 or 8 poles that are not Ex-eb increased safety motors should meet at least IE3 efficiency. Motors that have output power greater than 120W and less than 750W with 2, 4, 6 and 8 poles that are not Ex-eb should meet IE2 efficiency. Whereas all VSD with rated output power greater than 120W and less than 1000kW should match IE2 efficiency standard.

By July 2023 all Ex-eb motors with rated power in range between 120W and 1000kW with 2 to 8 poles must meet IE2 requirement. Similarly single-phase motors with rated output

² “Ex-eb” -increased Safety motors are certified for installation in hazardous areas

power equal or greater than 120W must match IE2. Whereas IE4 efficiency requirement will be compulsory for three phase non-Ex-eb motors with rated output power greater than 75kW up to 200kW with 2 to 6 poles.

Overall summary of the recent MEPS updates for motors and drives are depicted on Fig. 3. It can be concluded that IE1 standard drives have fall off the efficiency acceptance list and now are not consider as a viable option according to regulations. IE2 standard drives will follow the same fate in the nearest future, whereas IE3 and IE4 will be more common for industrial drives for rated power ranges between 120W and 1000kW. In this context, SynRM matches well the future drives requirements and soon will be widely adopted by most manufacturers.

III. PROBLEM WITH PERMANENT MAGNET MATERIALS

PMs are an essential component of the modern synchronous motors and generators. Key properties of PMs are coercivity and the remanent flux density. These are strongly dependent on the microstructure of the material itself. One of the most widely used PMs for traction motors and power generators contain Neodymium (Nd) and Dysprosium (Dy). Dy is used to sustain the NdFeB PMs coercivity at higher temperatures [36]. Both Dy and Nd are considered as Rare Earth Elements and listed as critical materials by US Department of Energy as well as the other international institutes due to the high risk in supply [37]. Other alternatives are the non-rare earth (non-RE) PMs which, although have lower magnetic performance, are still attractive for many applications where cost saving is a priority.

The request for NdFeB PMs has been significantly increasing due to the demanding needs of modern drives applications: higher energy efficiency, performance and power density. Fig. 4 presents the average price of Dy_2O_3 and Nd_2O_3 according to USGS Mineral Commodities Summaries. The average price of the Dy Oxide has spiked from 245\$/kg in 2010 to 1410\$/kg in 2011, then gradually went down to 185\$/kg in following 5 years. The price of the Nd Oxyde has also raised from 88\$/kg in 2010 to 195\$/kg in 2011, and then went also down to 39\$/kg [38]. The increase in Nd Oxyde average price was mainly caused by huge increase in demand in REE as well as the

monopoly of the critical REE mines in specific areas of the globe. After 2016, there has been an obvious divergence in the price of the two oxides shown in Fig. 4. This happened due to successful reduction of usage of the Dy element. In addition, China and biggest European countries are currently forcing the Electric Vehicles (EVs) market to replace the internal combustion engines, which are expected to be phased out in two decades. With the increase in number of EVs the Nd price will continue to grow and this constitutes the main driver for the industrial interest in REE free PM and electrical machines.

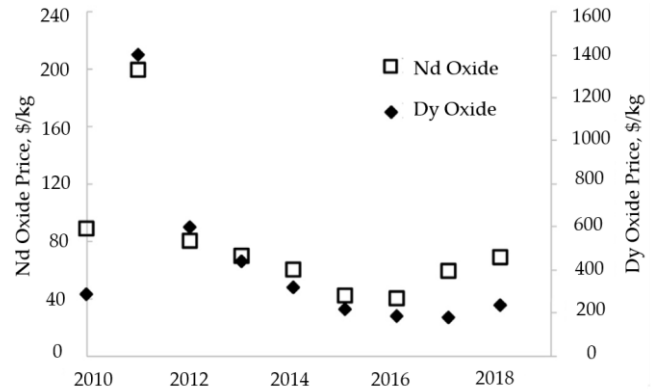


Fig. 4. REE Oxides price trends. The data was retrieved from the USGS Mineral Commodities Summaries [38], [1].

Based on the market report that was presented in [39], in 2015 the sale of NdFeB, SmCo, Ferrite and Alnico are 2927M\$, 722M\$, 4344M\$ and 355M\$, respectively. According to the PM sales report, Ferrite is dominant by occupying nearly half of the market. Ferrite PMs are very popular for motors that do not require high power densities. However, for those applications that are limited in size and weight i.e. aerospace application or EVs, REE magnets are the only viable choice. The most pragmatic approach to reduce the usage of REE is developing of non-REE magnets that can fill the magnetic performance gap between Ferrite and REE magnets [47]. Table I presents the prices and properties of the various PMs in 2016 as well as the predicted values in 2022. The table presents the cost properties ratios \$/kg/kG/kOe where the magnet cost per kg \$/kg is divided by the remanent magnetization kG and the

Table I. Comparison of PM prices and their properties. [47]

	$(BH)_{max}$ (MGOe)		H_{ci} (kOe)		Br (kG)		Price (\$/kg)	
	2016	2022	2016	2022	2016	2022	2016	2022
NdFeB (NH42SH)	40-42	42	20	20	13-13.3	13	60\$	120\$
Sm-Co (SC-3215)	31-32	34	15	15	11.2-11.8	12	128\$	210\$
AlNiCo-9	9	11	1.4	2	10.5	10.5	71\$	80\$
Ferrite (Sr-8B)	3.8	3.8	3	3	4	4	4\$	4\$

coercivity kOe. It is desired to develop non-RE magnets that will have higher value of cost property ratio (\$/kg/kG/kOe).

The strategies to address the REE problem are increasing and diversifying the supply sources and reducing the demand. China, Australia, US, Vietnam have started to open new REE mines including the Dy ones. However, none of the newly opened mines can compete with the existing ones that are rich in REE deposits which are mostly based in China. To reduce the demand in REE, non-RE or less-RE PM technology are being investigated. Significant advancement in reducing Dy content in NdFeB, while still keeping high level of coercivity, was achieved by the reduction of the grain size of the PM [41]. The development of the EM technologies that does not require the PMs field is one of the key approaches to solve the described problem.

Another major drawback of REE is that sourcing and processing is very carbon intensive and recycling is still immature. In [42], an in-depth analysis of REE PMs is given, highlighting their impact on the environment. Indeed, in order to make REE PM more environmentally sustainable there is a need to push towards recycling solutions.

In summary, it can be concluded that the current trends towards higher efficiency as well as REE-free technologies makes EMs based on the reluctance principle a serious alternative. The rapid industrial acceptance of the SynRM is a matter of time, as the biggest motor manufacturers and R&D institutions are working towards the described challenges.

IV. OPERATING PRINCIPLES OF SYNCHRONOUS RELUCTANCE MACHINES

In this section the operating principles of SynRM is compared with other synchronous machine topologies. Reluctance torque, also known as alignment torque, is due to the forces that occur when a magnetic material interacts with a magnetic field. The torque produced in SynRM is caused by unequal magnetic permeability in the transverse and longitudinal axes of the rotor that has no windings or permanent magnet excitation. The AC current flowing through the stator windings creates a rotating magnetic field in the air gap of the motor that rotates at synchronous speed, the rotor follows the

magnetic field without reaching magnetic field itself, therefore the machine continuously produces torque.

Reluctance motor described within the synchronous d - q reference frame, the d - axis is considered the path of lower reluctance (high flux-to-MMF ratio) while the q - axis is the path of higher reluctance (since the flux-barriers obstructing the flux). Therefore, the saliency ratio ξ , defined as the ratio between the d - and q - axis inductances has to be maximized [12].

A. Synchronous topologies classification:

Synchronous machines can be also classified based on their torque production phenomena: PM torque and reluctance torque. PM torque is the torque that occurs between two interacting magnetic fields, i.e. PM machine having rotor field

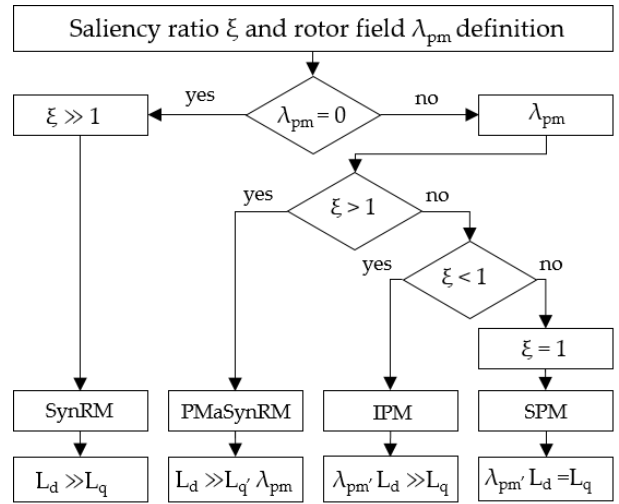


Fig. 5. All possible combinations of reluctance and PM torque components. [1]

produced by permanent magnets and stator field generated by stator currents. [43], [12].

Fundamental torque equation for cylindrical machines in d - q frame, represents both phenomena:

$$T_{dq} = 1.5p[(L_d - L_q)i_d i_q + \lambda_{pm} i_q] \quad (1)$$

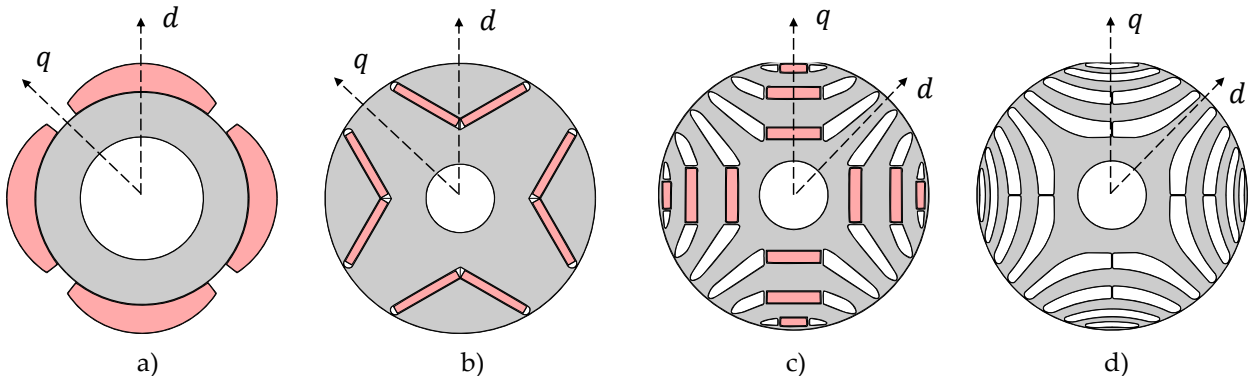


Fig. 6. PM to reluctance machine topologies [1].

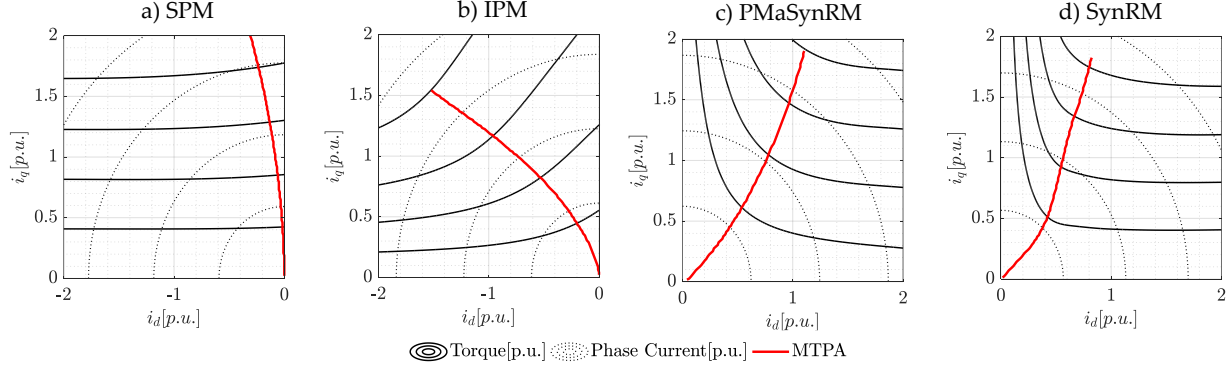


Fig. 7. Constant torque curves with highlighted MTPA trajectory on the (i_d, i_q) plane [1].

where $(L_d - L_q)i_d i_q$ is the reluctance component, and $\lambda_{pm} i_q$ is the PM part. The relative proportion of the PM and reluctance torque components will depend on the amount of PM (or any other rotor field source) and the amount of rotor's magnetic saliency. Hence, there is huge number of possible combinations that can be applied in (1) [12]. An effective way to visualize the classification of synchronous machines is shown in Fig. 5. Here, the saliency ratio quantifies the capability of the reluctance torque. Saliency ratio is defined as:

$$\xi = L_d / L_q \quad (2)$$

Fig. 5 highlights 4 main synchronous machine topologies. SPM is a surface mounted PM machine, which has “no saliency” ($\xi=1$). This topology contains pure PM torque (1). IPM is an interior PM machine, it has saliency however, mainly relies on PM torque component. PM assisted synchronous reluctance machine (PMaSynRM) that is designed in such way, that machine mainly rely on reluctance torque component. Whereas SynRM is a pure reluctance torque machine. All 4 rotor topologies are presented in .

The common way of representing the d - q axis for synchronous machines is that d -axis is always the axis of the higher flux. In fact in PM machine the main flux is given by the PM's Fig. 6 a) and b), while in reluctance machine it is where permeability is higher Fig. 6 c) and d) [44]. As can be observed on Fig. 6 a) surface PM rotor exhibit no saliency, this rotor topology has a uniform iron rotor, whereas the permanent magnets are mounted on top of it. Hence the magnetic permeability of d and q axes is ideally uniform ($L_d=L_q$), when the machine is not highly saturated. In general, the inductances of the surface mounted PM is quite low, since the magnet has very low relative permeability. Hence the magnets, which are mounted on the rotor iron surface increase the effective air gap length. The magnets are exposed directly to the armature field, hence are subject to partial irreversible demagnetization [45].

The IPM rotor has the magnets buried in rotor lamination Fig. 6 b), hence introducing saliency, as the rotor iron geometry is non-uniform. The magnetic conductivity of d and q axis is not equal, as the magnets that are placed in q -axis direction have a much lower magnetic permeability compared to the iron ($L_q > L_d$). Multilayers of magnets can be used to further increase

the saliency. One of the advantages of the IPM are that the magnets are effectively shielded from the demagnetizing armature field during the flux weakening operation [46]. Since $L_d < L_q$, these machines usually operated in the second quadrant of the (i_d, i_q) plane. As discussed in [46], the q -axis inductance is usually higher compared to an equivalent SPM, therefore generally IPM are more suitable if a wide constant power speed range is desired. Indeed, the constant power in flux-wakening mode of operation is achievable at lower Volt-Amps ratings compared to surface mounted PM machine [47], [48], [49].

PMaSynRM rotor as shown on Fig. 6 c) usually (but not always) has weaker magnets or lower magnet volume, hence indicates less PM torque compared to IPM. However, it has much higher saliency due to higher number of flux barriers. The interior flux barriers are placed in q -axis direction ($L_d > L_q$). In order to increase the reluctance torque component, the rotor anisotropy is maximized by introducing more than one flux barrier [50]. This topology shares similar features with IPM, in terms of constant power achieved during flux-weakening operation. This machine topology mainly rely on the reluctance torque component, and it exhibits several drawbacks related to the torque ripple, low PF and mechanical constrains related to the flux barriers retention [21], [51].

Pure SynRM rotor has no magnets, hence exhibits no PM torque. This topology has much higher saliency ratio along the q -axis compared to other topologies ($L_d > L_q$) [52]. Similarly to PMaSynRM, SynRMs feature demanding rotor mechanical constrains and higher torque ripple. Due to the presence of the iron ribs which physically hold the whole rotor structure together, the cross-saturation effect occurs [53], [54], as the d and q rotor axis are not completely magnetically isolated due to presence of shared flux path area such as the iron bridges. Hence, an accurate FE-evaluation of the machine electromagnetic performance is required.

B. Torque performance comparison

To better visualize the torque operation of different synchronous machine topologies, the constant torque curves are presented in Fig. 7 in p.u values.

As can be observed in Fig. 7 a) the SPM torque performance depends only on i_q , however at higher currents the Maximum Torque Per Ampere (MTPA) control strategy requires a

negative i_d . This happens because the d -axis inductance saturates at lower currents with respect to the q -axis one.

Since IPM has both reluctance and PM torque components (Fig. 7 b), it requires both i_d and i_q currents to follow the MTPA. Since the d -axis inductance is smaller than q -axis inductance, higher torque is achieved with the negative i_d . The torque curves are dependent on both i_d and i_q , therefore a detailed electromagnetic analysis or experimental identification required to derive the MTPA look up table. [55]

The PMSynRM topology, (Fig. 7 c), operates in the first quadrant as the d -axis inductance is greater than the q -axis inductance. As can be observed, the PMSynRM torque curves are somewhat mirroring the IPM torque behavior with respect to the i_q axis; however, the MTPA is inclined towards the i_q axis. It is important to note that for this topology the rotor q -axis is aligned with the magnet, hence the i_d is required to get PM torque (Fig. 7).

As can be observed from Fig. 7 d), the SynRM MTPA trajectory is further inclined towards i_q axis compared to PMSynRM, as there is no PM torque component. The SynRM's torque curves are highly dependent on d -axis inductance saturation levels, whereas it is desired to minimize the q -axis inductance. It can be observed that the SynRM, PMSynRM and IPM torque profiles are more current angle dependent as the MTPA trajectory change rapidly. This is caused due to the salient nature of the rotor, meaning torque is entirely or partially produced by reluctance torque, due to interaction of the stator currents with the anisotropic rotor structure. Its operating principle is thus highly dependent on the saturation levels of the iron material. Based on these it can be said that the current phase angle will vary considerably with respect to the current-torque levels of the operating instance, which leads to a relatively complex control strategy. However, in the past decade, it has been demonstrated that both sensorless and sensorless implementation is possible thanks to the knowledge of the machine's electromagnetic model [12] [56].

The above considerations justify the slower adoption of SynRM, which presents some challenges requiring a more complex control strategy compared with PM machines. This can be considered one of the historical main barriers to the wide industrial acceptance of SynRM since it requires a more expensive drive and control platform needed to implement the more complex control algorithms.

V. STATE OF THE ART

This section discusses the research works that contributed to address the main design challenges of the SynRM.

The rediscovery of the SynRM and their design challenges started in the early 90s. Important works related to the SynRM geometry and design procedures were addressed by the pioneering works of Vagati [57], [58], [59], [60]. In particular, in [57] a SynRM drive was compared with Brushless REE PM machine and IM. It concluded that SynRM has a great potential in industrial sector as it can achieve a relatively high torque density at a competitive cost.

A. Key design challenges

Historically the main streams of the research works have been covering the SynRM design challenges: maximizing average torque [4], [61], [62]; minimizing torque ripple, [63], [64], [21], improving the power factor (PF) [63], [65] and the comparison with other topologies, [4], [61], [66], [67],[68],

In [58] the main problems of the SynRM design were outlined highlighting for the first time all the compromise of the reluctance torque production, namely the maximization of the anisotropy, the magnetizing flux and q -axis current. Different rotor and stator structures were investigated. In this work, for the first time the mechanical problem associated with the ribs was also highlighted. In [59], the SynRM torque ripple was analytically evaluated and the effect of the barriers' angular position at the airgap on torque ripple was studied. The concept of the "equal pitch" rotor flux barrier distribution, as shown in Fig. 8, featuring multiple iron segments was first introduced and analysed. Another work addressing the identification of the optimal rotor geometry for low torque ripple was presented in [60], and it aimed to outline a general design approach.

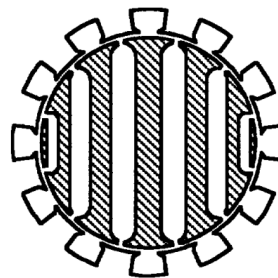


Fig. 8. "Equal pitch" rotor for 2-pole configuration. [59]

One of the early rotor design optimization methods of SynRM was presented in [69]. The key objective of the optimization was to improve the PF. It was proven that the PF of 0.8 is a practicable achievable value. In [70] various factors affecting the saliency ratio were investigated. It was shown that the rotor design and in particular the number of barriers have the most significant impact. Indeed, maximizing the number of rotor barriers increases the saliency ratio although there is a physical limit to their maximum number.

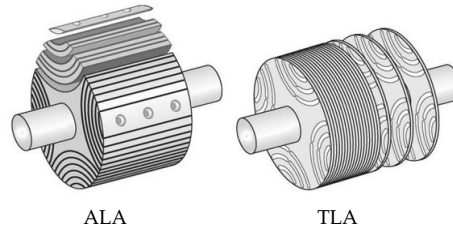


Fig. 9. ALA and TLA SynRM topologies. [71], [72].

Higher number of barriers can be achieved by adopting axially laminated rotor (ALA). The main difference between conventional transverse laminated rotor (TLA) and ALA is in the manufacturing process. Fig. 9 shows the assembly process of the ALA and TLA topologies. As can be seen, the ALA rotor is assembled by placing the iron rotor pieces axially kept by pole holder bolts. Whereas the TLA is conventionally

assembled by stacking rotor lamination together. It was proven in [73] that ALA topology can significantly improve the performance by increase in saliency, PF and torque capability. An example of an ALA SynRM rotor is reported in Fig. 10.

Even though ALA topology seems to have several superior features that comes from the significant increase of the barrier numbers, it is still has issues limiting its commercialization. The problem associated with increased iron losses of this topology is considered a minor drawback, nevertheless it significantly limits its efficiency advantages. Challenges of the manufacturability plays a more important role, as the ALA is more difficult to assemble when compared to the conventional TLA structure [12].



Fig. 10. Assembled ALA rotor topology. [73]

In terms of manufacturing for a high-volume production, where the lamination cutting is done by punching techniques, the TLA manufacturing difficulty can be considered equivalent to IPM machines where the retention of the rotor structure and PMs is done by iron ribs.

B. Complex geometry

Based on all the above, it can be stated that the main machine design challenge comes from the fact that SynRM has a very complex structure, therefore many geometrical parameters are involved in the machine sizing and optimization. Many works have attempted to address the rotor complexity as in [61], [74], [75], [76], [52].

One of the recent SynRM rotor design method that is currently widely used was introduced in [77]. The goal of this work was to introduce an easy approach of the design and optimization by a comprehensive parameterization of the rotor geometry as highlighted in Fig. 11.

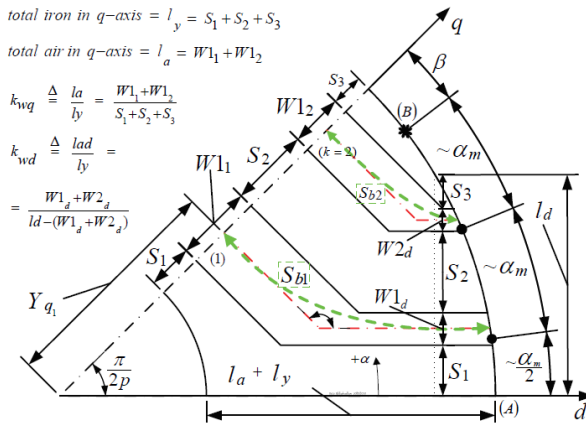


Fig. 11. Rotor geometry and related microscopic and macroscopic parameters [77].

Various analytical methods usually based on the lumped magnetic circuit of the machine are used to identify the optimal distribution of air insulation along the q -axis of the rotor [52], [71]. However, time-consuming Finite Element based optimization is still a necessary step to address the optimization of the main performance indexes (torque ripple reduction, loss reduction etc.). The SynRM rotor complexity naturally increases the time and the steps that are required during the design optimization stage [78], [79], [76], [21].

The computation time varies according to which performance targets are being optimized (torque, torque ripple, iron losses, etc.) and [21], [22], [80], [81] have investigated the problem of establishing the trade-off between accuracy and computational burden.

On the other hand, the geometrical complexity of the problem can be further reduced acting on how the rotor geometry is parametrized. In particular, [81] and [64] present a comparative study among different SynRM flux barrier parametrizations, analyzing the compromise between geometrical complexity, achieved performance and computational time. It is a general conclusion that adopting a flux barrier profile described by the Joukowski equation and a flux barrier parametrization described by three parameters (barrier thickness, air gap angle and end-barrier parameter) is the best compromise between performance and geometrical complexity [64], [77]. These parameters are also the ones, which most affect the torque performance, and for this reason they usually optimized during the FE refinement stage.

C. Accurate analytical sizing

A preliminary analytical sizing is usually the first step of any EM design procedure. In this step the machine general dimensions are determined [82], [83], [84]. The classical sizing approach of a SynRM relies on the torque relation for common cylindrical machines derived from the magnetic field energy at the EM's air gap whose general expression is:

$$T \sim V \cdot B \cdot A \quad (3)$$

Here T is torque, V is the rotor volume, B is the air gap flux density usually referred to as the magnetic loading and A is the linear current density referred as the current loading.

A novel sizing approach that is capable to consider the EM's rotor salient nature was introduced in [85]. The saliency (2) was derived by considering the magnetizing coefficients of both d and q axes, that quantify the magnetic conductivity of the respective axes [71]. The saliency can be then derived as:

$$\xi = \frac{L_d}{L_q} = \frac{L_{dm} + L_l}{L_{qm} + L_l} = \frac{L_m K_{dm} + L_m K_{qm}}{2L_m K_{qm}} \quad (4)$$

where L_m is the magnetizing inductance, L_l is the leakage inductance and K_{dm} and K_{qm} are d and q axis magnetizing coefficients. The main assumption is that L_{qm} is assumed to be associated with leakage flux. Therefore, $L_l = L_{qm}$.

In [85] the general dimensioning equation was derived considering the salient nature of the machine using equation:

$$D_{ro} = \sqrt{\frac{T \gamma \mu_0 q K_{dm} \sqrt{\xi}}{B_{1d}^2 \pi g \sqrt{1 + \left(\frac{1}{2\xi} - 1\right)^2 \xi}}} \quad (5)$$

Where the D_{ro} is the rotor diameter, q is the number of slots per pole per phase, g is the air gap length, μ_0 is the relative permeability of free space While the aspect ratio, γ is defined as:

$$\gamma = \frac{L}{D_{ro}} \quad (6)$$

being L is the stack length.

D. Torque Ripple optimization

In [77] a novel fast and systematic design procedure for SynRM was introduced. The average torque and torque ripple optimization workflow revolves around finding the best combination of barriers geometries and stator geometrical parameters. Three design parameters are considered, which are the insulation ratios in q – axis, the barriers angles distribution and stator geometrical parameters. These are highlighted in Fig. 12.

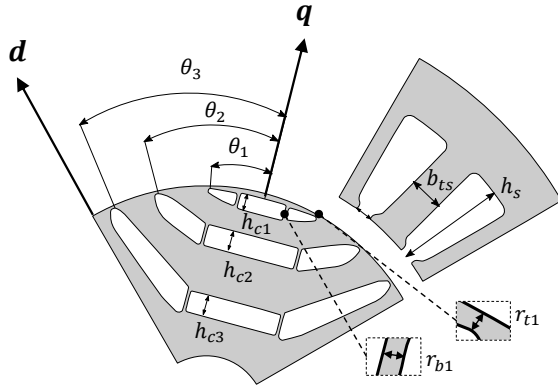


Fig. 12. Sketch of a typical SynRM geometries with highlighted key geometrical parameters [86].

The insulation ratio [12], [86], [85] is defined as the total thickness of the magnetic insulation typically air in q -axis with respect to total thickness of the rotor lamination as:

$$k_{air} = \frac{\sum_k h_{c_k}}{R_{ro} - R_{sh}} \quad (7)$$

Where R_{ro} is the rotor radius and R_{sh} is the shaft radius and h_{c_k} is the barrier' thickness in q -axis direction.

An analytical model was developed in [87] to study the effect of the SynRM rotor geometry on the torque harmonic. Various automated optimization techniques were studied in [88]. Multi-objective Genetic Algorithm (MOGA), Multi-objective Differential Evolution (MODE) and Multi-objective Simulated Annealing (MOSA) were evaluated considering two objectives: torque ripple and average torque. It was identified that MODE gave the best results with less computational burden. In [89], a sensitivity analysis of torque ripple reduction was performed on SynRM as well as the PMaSynRM. It was shown that a small variation in rotor geometry can cause a high torque ripple. A single objective optimization (SIMPLEX) was carried, and the optimal solution was further studied at different current ratings.

Indeed, the torque ripple is one of the key drawbacks of the SynRM topology, however it has been shown that it can be effectively addressed by applying various design optimization techniques. There are various example in key journal publications showing that torque ripple can be minimized up to values lower than 15% [77], [89], [88], [90].

E. PM assistance

PM assistance is the main design leverage to improve the SynRM PF [12], [63], [65]. A single PM piece, usually Ferrite is inserted into the rotor flux barrier central segment as shown in Fig. 13 [91].



Fig. 13. PM insertion. SynRM to PMaSynRM [91].

A PM insertion results into reduction of the L_q (1), as the PMs tend to saturate the iron bridges, ribs and the obviously increase in PF as the presence of the PM's flux linkage compensates the $L_q I_q$ as shown in the Fig. 14.

The PF improvement leads to reduction of the required Volt-Ampere rating of the power electronics converter with a significant cost savings. Moreover, PM assistance will improve a field-weakening (FW) capability as it was highlighted in [12]. By solving phasor diagram (Fig. 14) the FW capability can be increased if the ratio between q -axis inductance and PM flux follows the relation (8) [49]:

$$\frac{L_q I_q}{\Lambda_m} \geq 1 \quad (8)$$

Where Λ_m is PM flux linkage as it is shown in Fig. 14.

In addition, the use of Ferrite magnets does not significantly affect the motor cost because of its low price, about 3.4 EUR/kg [12].

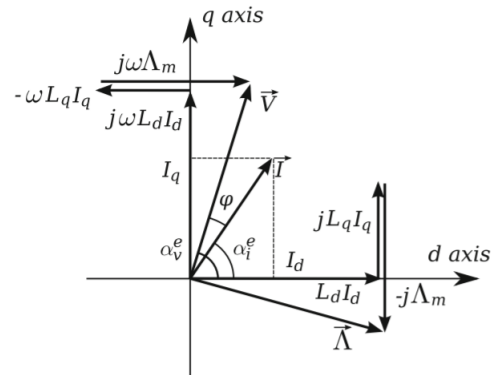
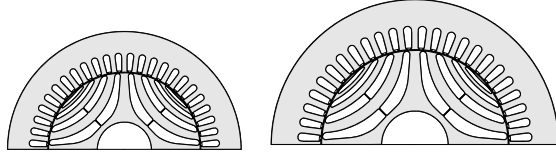


Fig. 14. Phasor diagram of PMaSynRM.

F. Homothetic design scaling principle

One of the recent advancements in the design methods for SynRM makes use of the homothetic scaling criteria. It has been proven that this approach is useful as preliminary design technique when sizing a wide range of machines [92], [93].

In [92], the design scaling principle was validated for a wide range of the machines. The main idea is that starting from an optimized SynRM geometry for a specific power rating, a wide range of other machines for different power ratings can be obtained by simply scaling the original optimal geometry. An example of scaled SynRM geometries is presented in Fig. 15.



M21 -----> M22
 $\cdot S_{si}=1.23$
 Fig. 15. Scaled SynRM M21 and M22.



Fig. 16. a) M21 and b) M22 SynRM experimental rigs [85], [93].

The behavior of the derived machines was studied using the methodology presented in [85], allowing to identify interpolating functions which correlate the machine sizes with its performance. Power Regression (PWR) and Polynomial Regression (PLR) methods were used to derive the following general equations (9):

$$T(R_{si}, \gamma) = p_0 + \sum_{k,j} a_k R_{si}^k + b_j \gamma^j + c_{k,j} R_{si}^k \gamma^j \quad (9)$$

Where R_{si} is the stator inner diameter, a_k , b_j and $c_{k,j}$ are i^{th} and j^{th} order specific PLR coefficients. Similarly, the constant torque curves on (i_d, i_q) plane were generalized with respect to ampere-turns as (10):

$$T_{pu}(mmf_d, mmf_q) \sim \sum_{k,j} a_k mmf_d^k + b_j mmf_q^j + c_{k,j} mmf_d^k mmf_q^j \quad (10)$$

Where mmf_d and mmf_q are the d and q axes magnetomotive forces respectively, whereas the T_{pu} is the per unit torque value

that is defined with respect to the torque value that occurs at the MTPA trajectory current phase angle of $\alpha^e=60^\circ$ as:

$$T_{pu} = \frac{T(mm f_{s1}, \alpha^e)}{T(mm f_{ref}, 60^\circ)} \quad (11)$$

Where mmf_{s1} is the stator fundamental magnetomotive force and mmf_{ref} is the reference magneto motive force for MTPA excitation current $\alpha^e=60^\circ$.

The proposed functions (9) and (10) were validated experimentally on two machines that were derived from the similar geometry both having 4-poles 48-slot combination labeled as M21 and M22 Fig. 16. M22W is a derived machine that was scaled radially by factor of $S_{si} = 1.23$ with respect to the original geometry M21.

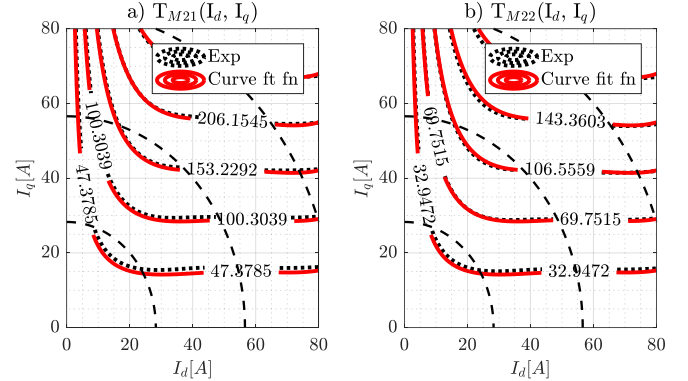


Fig. 17. Comparison of constant torque curves on (I_d, I_q) [93].

Fig. 17 presents the constant torque curves comparison of the derived with the interpolating function (10). As can be observed both machines have a very similar torque patterns, which confirms the proposed scaling design approach.

In [92] the effect of homothety was also evaluated in terms of torque ripple. Two general sizing approaches based on the homothetic scaling principles were defined and evaluated. It was shown that the rotor parameters converge to the same per unit values for all the scaled geometries. It was shown that the FE design stage can be greatly simplified by considering a novel dimensioning techniques.

G. High speed SynRM

High speed (HS) SynRMs have attracted an ever increasing research interest in the last decade. The key publication in that matter are [94], [95], [96], [97], [98], [99], [100].

A comprehensive study of the HS-SynRM was performed in [96], stator and rotor laminations are shown on Fig. 18. The HS-SynRM was designed in two stages considering electromagnetic and mechanical optimization.



Fig. 18. Stator and rotor laminations [96].

It can be said that the key challenge for the high-speed applications is optimizing from both electromagnetic and structural point of view the rotor geometry in order to guarantee the integrity of the rotor at high speeds and minimize the unwanted leakage flux caused by ribs thickening and so the related torque loss. In [95], a comparative design exercise of different rotor of HS-SynRM was presented considering both electromagnetic and structural aspects. The trade-off between rotor geometrical complexity, optimal performance and computational burden was deeply investigated. The designed machine was manufactured and tested reaching 35,000 rpm. The efficiency as reported to be always above 80%.

In [99], a comprehensive design methodology for HS-SynRM has been introduced and validated against FEAs and experimental findings. Adopting the same design approach, [100] reports a comparative design exercise in order to identify the optimal soft magnetic materials to be used for both stator and rotor of a HS-SynRM.

In [94], two pole SynRM (shown in Fig. 19) with minimized eddy current losses were designed. The rotor was assembled of bonded segments of ferromagnetic and non-magnetic steels. Experimental results proved to reach a 10kW 10,000 rpm with 91% efficiency, whereas the rotor/losses had 0.5% of the total input power.

In brief it can be said that SynRM has a potential for high-speed application. The main challenge comes from the mechanical aspect, which was proven to be effectively addressed with a multi-physics design approach.

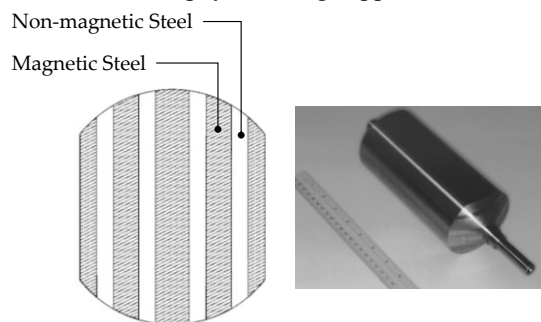


Fig. 19. HS-SynRM, rotor structured on the left side, assembled rotor on the right side [94].

For the past three decades there was a strong research push towards the SynRM industrialization. A number of innovative design techniques were developed and successfully utilized to address the main design challenges of the topology. It can be concluded with confidence that the SynRM design is no longer can be considered as a very complex procedure thanks to the research contribution. The design procedure has been “standardized” for the easiest and fastest way for the development of the optimal SynRM.

VI. SYNRM POTENTIAL AS A MODERN INDUSTRIAL EM

In order to better understand the potential of SynRM technology, a detailed comparison with SCIM and PM machines is hereafter reported highlighting advantages and drawbacks.

A. SynRM vs SCIM, SynRM vs PM machines

A common design practice for the SynRM is to use the stator of SCIM and simply substitute the rotor. In [101], it was shown that approximately 80% of torque can be retained whereas the losses were reduced down to 60% of initial design adopting this design approach making the SynRM a valuable alternative for industrial application [102]. The SCIM has been serving as the *industry’s workhorse* for over a century, high-efficiency SynRM it is a competitive technology that could be a replacement of SCIM in many applications. The following SynRM advantages over SCIM can be highlighted as [101], [102]:

- + Synchronous operation – no slip, synchronous drive
- + No conductors in rotor
 - o Robustness
 - o Manufacturing cost
 - o Less rotor losses
 - o “Cold” rotor
 - o Lower maintenance requirements
- + Higher efficiency
- + Potentially higher power density within the same frame size
 - + Lower rotor inertia
 - + Longer bearing life

Main improvements with respect to SCIM come from the fact that SynRM has no conductors in rotor, which brings many benefits from design and maintenance points of view. In general, it is estimated that approximately 25% of total losses in SCIM is coming from the rotor. It is well known that in any EM, the rotor is the most difficult part to cool. Hence, this leads to conclusion that the SynRM is a “cold rotor” machine [80], [10]. Majority of SynRM losses are generated in the stator (copper losses), where the heat is generally easier to remove with classical finned frames. Nevertheless, along with the highlighted advantages the disadvantages of SynRM with respect to SCIM can be highlighted as:

- No line-start-up capability (unless considering line start SynRM)
- Lower power factor [70]
- Complex control
- Not yet widely accepted by industry

Comparing PM synchronous machine and SynRM, both have similar operation principles and do not contain any rotor conductors. Hence, the rotor losses are reduced compared to SCIM. However, the rotor’s field is produced by permanent magnets which can be the source of other loss (i.e. eddy current losses in the PM). There is no doubt that the PM machines have superior torque density. However, there are number of advantages of SynRM over PM machines:

- + No PM
 - o Significantly reduced cost
 - o Significantly reduced embedded carbon
 - o Easier assembly and manufacturing
 - o Significantly reduced risk of overvoltage
 - o Reduced risk in supply chain
- + Robustness (No PM demagnetization risk)

- + Wider operating speed range
- + No need of disengagement mechanism (clutch) in case of short circuit faults

Lack of PMs are the main advantage of the SynRM which brings a lot of benefits. Apart from cost reduction and manufacturing benefits such as reduced embedded carbon (skipping PM manufacturing stage), lack of PMs in rotor eliminates the risk of over-voltage. It can occur in field-weakening operation at higher speed. In case of control loss, back EMF generated by motor at higher speed can easily damage the inverter [103].

Nevertheless, the PM machines still have obvious advantages over SynRM. SynRM is expected to have:

- Lower power density and torque density
- Lower power factor
- Increased VA ratings
- Non constant power speed range

Considering the example of the ABB's product line which includes SCIMs and PM motors as well the SynRM, the SCIMs are capable to meet the IE2 to IE4 standards up to 1200kW. The PMs are mainly aimed for higher torque dense solutions up to 2500kW. Whereas the SynRM is aimed to fill the gap in performance and efficiency between conventional SCIMs and PM machine [32], [19]. The main advantages of the SynRM that are listed by ABB are lack of any rotor excitation (no winding or magnets) as well as the service-friendliness respect with an SCIMs as there is no magnetic forces in rotor. One of the most recent advancement according to [32], is the new IE5 SynRM drives. These motors meet the requirements of the IEC 60034-30-2 and are produced for a power range between 5.5 to 315kW.

Several advantages of SynRM over SCIM and PM machine were discussed by [12], [10], [104]. In summary, SynRM has higher efficiency compared to SCIM and significantly lower price compared to PM machines thanks to lack of rare earth materials. Considering a rotor with no conductors and permanent magnets translates in better robustness and less losses. Also, it has noticeably wider speed range compared to PM machine [105]. Therefore, SynRM is a promising alternative to SCIM and PM machines. Biggest challenges can be highlighted as high torque ripple and lower power factor also due to the iron ribs required for mechanical retention [106].

B. Qualitative cost comparison

A qualitatively cost analysis of SCIM, PMaSynRM and SynRM has been reported in [107]. The comparison was carried out for a same stator frame and slot/pole combination. Four different motors were considered: SCIM with copper and aluminum bars, SynRM and PMaSynRM machine with the ferrite PMs. The comparison includes the price of the raw materials only which was provided by manufacturers partners and does not include the cost of the manufacturing.

The comparison was carried out under assumptions that all four motors have same stator geometry and non-active electromagnetic components such as shaft, bearings and housing parts. In this example the M470-35A electrical steel was used in accordance with EU Standard EN 10106 [108].

Table II summarizes the comparison in terms of weight and cost of the raw material including the price in USD/kg as of April 2021. It is important to outline that the specific cost of materials will vary depending on manufacturer.

Based on the summary of Table II, SynRM rotor is the cheapest topology as it is essentially "one iron piece" rotor. The PMaSynRM is approximately three times more expensive due to additional cost of ferrite PMs. Nevertheless, considering benefits that are brought by PM insertion, as it was discussed in Chapter V - E, it can be a valuable solution for certain applications. Copper bar SCIM (Cu) topology have significantly increased price compared to the other alternatives. Whereas Aluminum bar SCIM (Al) have two-time cost of SynRM.

To conclude, SynRM rotor have reduced price compared to the other main contenders, therefore, it represents the most economical option for a large-scale industrial production.

Table II. Qualitative cost comparison. [107]

Raw Materials Properties				
Raw material	Mass density [kg/m ³]		Cost [\$/kg]	
<i>Ferromagnetic steel (M470-35A)</i>	7650		1.67	
<i>Cu bars</i>	8900		9.23	
<i>Al bars</i>	2950		4.55	
<i>Ferrite PMs</i>	4800		3.28	
Weight [kg]				
Component	Rotor type			
	SCIM (Cu)	SCIM (Al)	SynRM	PMaSynRM
<i>Rotor lam.</i>	0.701	0.701	0.679	0.679
<i>Cu bars</i>	0.673	-	-	-
<i>Al bars</i>	-	0.278	-	-
<i>Ferrite PMs</i>	-	-	-	0.058
<i>Total weight</i>	1.374	0.979	0.679	0.737
Cost [\$/kg]				
Component	Rotor type			
	SCIM (Cu)	SCIM (Al)	SynRM	PMaSynRM
<i>Rotor lam.</i>	1.17	1.17	1.14	1.14
<i>Cu bars</i>	6.22	-	-	-
<i>Al bars</i>	-	1.27	-	-
<i>Ferrite PMs</i>	-	-	-	2.41
<i>Rotor cost \$</i>	7.39	2.44	1.14	3.55

C. Line-Start SynRM

A direct-on-line topology of SynRM or Line-Start SynRM (LS-SynRM) have been widely developed for many applications such as fans, compressors and pumps [109], [110] [111], [112]. One of the main reasons LS-SynRM is getting wide attention is the ability to line-start just like SCIM without the need of an inverter. Also, the secondary copper losses of

SCIM can reach up to 25% of total losses [109]. Therefore LS-SynRM is a perfect candidate to replace standard SCIM.

In [110], [111] a full comparison of three different LS-SynRM with SCIM was presented. Rotor topologies of LS-SynRM had different approach in barrier and rotor cage positions as shown in Fig. 20. As can be observed, SynRM flux barriers were filled with the aluminum (dark gray). These three LS-SynRM topologies were tested in comparison with the equivalent SCIM. Summary of the steady state performance at rated conditions are shown in Table III, where LS-SynRM1 is Fig. 20 a), LS-SynRM2 is Fig. 20. b) and LS-SynRM3 is Fig. 20. c)

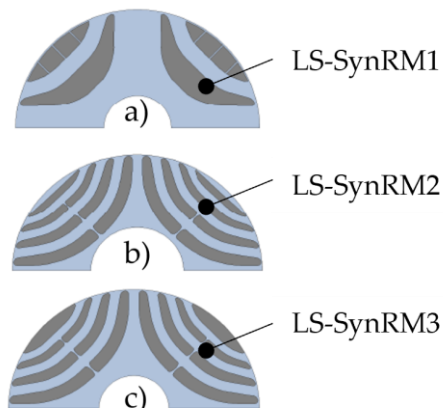


Fig. 20. LS-SynRM rotor topologies [111].

As can be observed LS-SynRM2 and LS-SynRM3 have higher efficiency in comparison with LS-SynRM1 and SCIM, which is mainly due to reduced Joule losses at rotor. However, all LS-SynRM machines have lower PF in comparison with SCIM which can be addressed by introducing a Ferrite PMs. [12], [111].

Table III. Summary of the steady state performance of LS-SynRM and SCIM. [111]

Parameter	LS-SynRM1	LS-SynRM2	LS-SynRM3	SCIM
Line voltage [V _{rms}]	398	398	398	398
Phase Current [A _{rms}]	5.8	4.79	4.95	5.0
Continuous Torque [Nm]	14.2	14.2	14.2	15.1
Rated Speed [rpm]		1500		1381
Rated Power [W]	2231	2231	2231	2183
Rated PF	0.718	0.763	0.745	0.794
Joule loss, stator [W]	439	299	318	330
Joule loss, rotor [W]	121	31	48	168
Efficiency [%]	77.3	84.5	83.4	79.0

VII. INDUSTRIAL ACCEPTANCE

In summary, the SynRM industrial acceptance has been steadily increasing over the last two decades as a main alternative to conventional SCIM.



Fig. 21. Losses and motor efficiency of the ABB's 37kW SCIM and the equivalent SynRM at rated conditions. (SynRM highlighted with blue, SCIM highlighted with black).

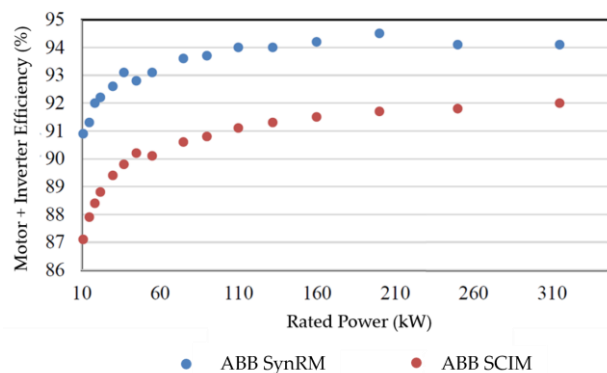


Fig. 22. SCIM and SynRM efficiency based on ABB's data, 2014.

A full product range of SynRMs, announced at a German motion control show in November 2012 by ABB. [19]. Currently, their high efficiency SynRM products range from 5.5kW to 350kW. Considering the machine design, SynRM can be sized for the exact same frame as an equivalent SCIM, however the achieved efficiency will meet the IE4 efficiency or even IE5. The same frame size SynRM can reduce the losses while delivering the same or higher power, which was demonstrated by ABB's offering [113]. These machines reduced in size and having a higher rated power and increased efficiency with respect to their SCIM counterpart.

Fig. 21 presents the losses comparison of the existing ABB's 37kW rated SCIM in black and SynRM in blue. As can be observed the SynRM efficiency reduction meets the IE4 standard with 95.3% - efficiency. Whereas the SCIM having a 92.7% efficiency falls under IE2 standard. The loss reduction for this motor example leads to 1.1kW power saving considering an 8760hrs of operation and having an average price of 0.15EUR/kWh leads to 1445 EUR/year savings.

To illustrate the superiority of the SynRM IE4 that is marketed by ABB, Fig. 22 is presented. The relative package efficiencies are depicted [19] (considering motor and inverter losses) over the offered rated power range for both SCIM and SynRM. Both SynRM and SCIM drives are at rated torque and speed, self-cooled, all machines are 4 pole 50Hz and controlled by ACS850 drive using sensorless direct torque control.

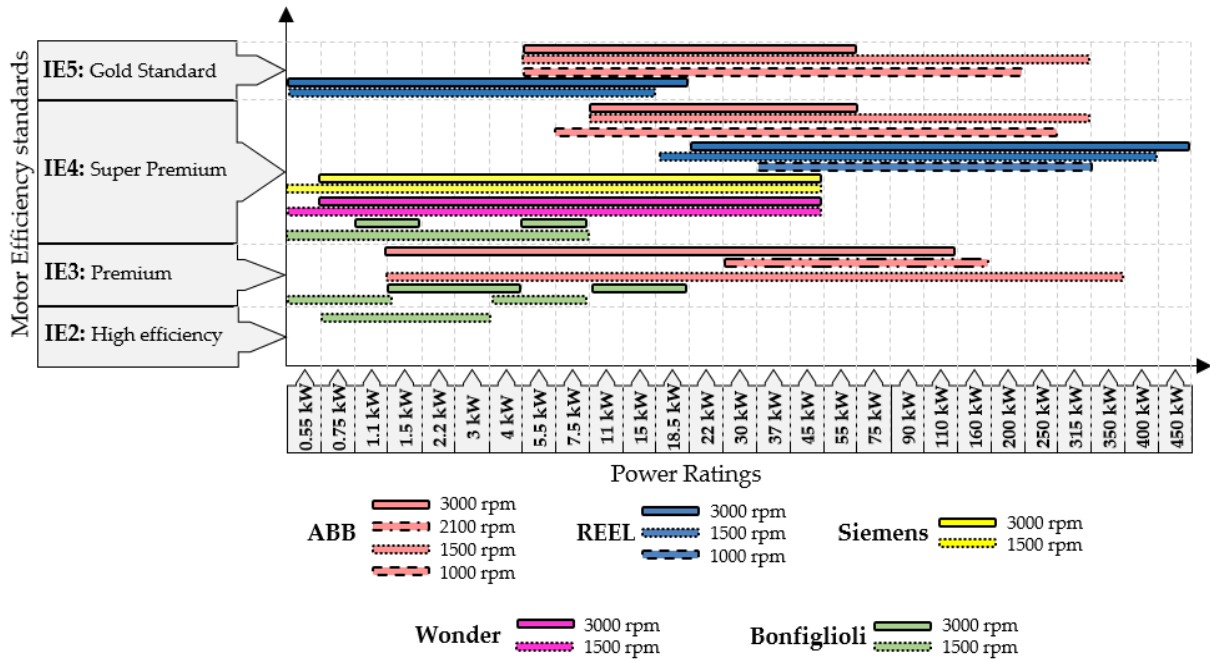


Fig. 23. SynRM process-performance motors that are available on the market as of Dec. 2020. All machines presented at rated speed and rated power.

As of December 2020, several EU motor manufacturers are already venturing towards the SynRM machines. Fig. 23 presents the SynRM line-ups of the key manufacturers as of Dec. 2020 based on the data gathered from [19], [20] [112], [113], [114], [115]. All manufacturers have various drives that meet IE2-IE5 efficiency standard. Bonfiglioli are currently producing IE2-IE4, lower rated machines that are rated at both 1500 rpm and 3000 rpm. They have different efficiency for machines rated up to 18.5kW. Wonder is another SynRM manufacturer that have a wider range of SynRM line up starting from 0.55kW up to 45kW for two rated speed options 1500 rpm and 3000 rpm. All machines are claimed to meet IE4 standard. Siemens currently having a very similar SynRM line up to Wonder from 0.55kW up to 45kW that meets IE4 standard.

The two biggest manufacturers are KSB REEL and ABB and they cover a very wide range of SynRM that can meet different efficiency standards. KSB REEL are dominant at lower ratings from 0.55kW up to 18.5kW, as claimed by the manufacturer these machines meet Gold Standard IE5. Whereas ABB has the IE3 machines for lower ratings. ABB are dominant at the power range starting from 7.5kW up to 315kW as they have a variety of the machines at different speed ratings: 1000 rpm, 1500 rpm, 2100 rpm, 3000 rpm that meet IE3-IE5. KSB REEL has the biggest power rated commercial SynRM products up to 450kW.

In conclusion, it can be stated that SynRM has seen an increasingly acceptance by industry and will continue to grow due to several related benefits.

VIII. ACKNOWLEDGMENT

Authors would like to thank the University of Nottingham Propulsion Futures Beacon for funding towards this research.

IX. REFERENCES

- [1] M. Murataliyev, "Novel sizing and modeling techniques for synchronous reluctance machines." Jul. 2021. [Online]. Available: <http://eprints.nottingham.ac.uk/64494/>
- [2] N. Bianchi, M. Degano, and E. Fornasiero, "Sensitivity analysis of torque ripple reduction of synchronous reluctance and interior PM motors," *IEEE Transactions on Industry Applications*, vol. 51, no. 1, pp. 187–195, 2015, doi: 10.1109/TIA.2014.2327143.
- [3] A. T. De Almeida, F. J. T. E. Ferreira, and G. Baoming, "Beyond induction motors—Technology trends to move up efficiency," *IEEE transactions on industry applications*, vol. 50, no. 3, pp. 2103–2114, 2013.
- [4] J. K. Kostko, "Polyphase reaction synchronous motors," *Journal of the American Institute of Electrical Engineers*, vol. 42, no. 11, pp. 1162–1168, 1923.
- [5] B. G. Lamme, "The story of the induction motor," *Journal of the American Institute of Electrical Engineers*, vol. 40, no. 3, pp. 203–223, 1921.
- [6] B. K. Bose, "A high-performance inverter-fed drive system of an interior permanent magnet synchronous machine," *IEEE Transactions on Industry Applications*, vol. 24, no. 6, pp. 987–997, 1988.
- [7] R. D. King, "Combined electric starter and alternator system using a permanent magnet synchronous machine." Google Patents, 1989.
- [8] G. Friedrich, "Experimental comparison between wound rotor and permanent magnet synchronous machine for integrated starter generator applications," in *2010 IEEE Energy Conversion Congress and Exposition*, 2010, pp. 1731–1736.
- [9] K. Miyashita, S. Yamashita, S. Tanabe, T. Shimozu, and H. Sento, "Development of a high speed 2-pole permanent magnet synchronous motor," *IEEE Transactions on Power Apparatus and Systems*, no. 6, pp. 2175–2183, 1980.
- [10] C. M. Donaghy Spargo, "Synchronous Reluctance Motor Technology: Industrial Opportunities, Challenges and Future Direction," *Engineering & Technology Reference*, vol. 44, no. May, pp. 1–15, 2016, doi: <http://dx.doi.org/10.1049/etr.2015.0044>.
- [11] T. Vaimann, A. Kallaste, A. Kilk, and A. Belahcen, "Magnetic properties of reduced Dy NdFeB permanent magnets and their usage in electrical machines," in *2013 African*, 2013, pp. 1–5.

- [12] G. Pellegrino, T. M. Jahns, N. Bianchi, W. L. Soong, and F. Cupertino, *The rediscovery of synchronous reluctance and ferrite permanent magnet motors: tutorial course notes*. Springer, 2016.
- [13] M. J. Kramer, R. W. McCallum, I. A. Anderson, and S. Constantinides, "Prospects for non-rare earth permanent magnets for traction motors and generators," *Jom*, vol. 64, no. 7, pp. 752–763, 2012.
- [14] J. H. Rademaker, R. Kleijn, and Y. Yang, "Recycling as a strategy against rare earth element criticality: a systemic evaluation of the potential yield of NdFeB magnet recycling," *Environmental science & technology*, vol. 47, no. 18, pp. 10129–10136, 2013.
- [15] A. T. De Almeida, F. J. T. E. Ferreira, and A. Quintino, "Technical and economical considerations on super high-efficiency three-phase motors," in *48th IEEE Industrial & Commercial Power Systems Conference*, 2012, pp. 1–13.
- [16] P. Waide and C. U. Brunner, "Energy-efficiency policy opportunities for electric motor-driven systems," 2011.
- [17] R. E. Machines—Part, "30-1: Efficiency classes of line operated AC motors (IE code)," *IEC Standard*, pp. 60030–60034, 2014.
- [18] E. E. Directive, "Directive 2012/27/EU of the European Parliament and of the Council of 25 October 2012 on energy efficiency, amending Directives 2009/125/EC and 2010/30/EU and repealing Directives 2004/8/EC and 2006/32," *Official Journal, L*, vol. 315, pp. 1–56, 2012.
- [19] "ABB SynRM Motors Without Rare Earth Magnets Deliver Ultra-Premium Energy Efficiency," *Magnetics*, Aug. 2020. <https://magneticsmag.com/abb-synrm-motors-without-rare-earth-magnets-deliver-ultra-premium-energy-efficiency/>
- [20] "REEL SuPremE® motor: Premium IE5/IE4 efficiency without magnets." https://www.ksb.com/REEL-en/products-solutions/Synchronous_reluctance_motors/reel-supreme-ie5/
- [21] M. Degano, M. Di Nardo, M. Galea, C. Gerada, and D. Gerada, "Global design optimization strategy of a synchronous reluctance machine for light electric vehicles," *IET*, 2016.
- [22] N. Bianchi and H. Mahmoud, "An Analytical Approach to Design the PM in PMAREL Motors Robust Toward the Demagnetization," *IEEE Transactions on Energy Conversion*, vol. 31, no. 2, pp. 800–809, 2016, doi: 10.1109/TEC.2016.2523556.
- [23] P. Bertoldi, "Recent development in energy efficiency policy in the EU," 2015.
- [24] A. de Almeida, F. Ferreira, J. Fong, and P. Fonseca, "Ecodesign Assessment of Energy-Using Products-EuP Lot 11 Motors," *Final Report for the European Commission*, 2008.
- [25] A. T. de Almeida, F. J. T. E. Ferreira, J. A. C. Fong, and C. U. Brunner, "Electric motor standards, ecodesign and global market transformation," in *2008 IEEE/IAS Industrial and Commercial Power Systems Technical Conference*, 2008, pp. 1–9.
- [26] A. T. De Almeida, F. J. Ferreira, and J. A. C. Fong, "Standards for efficiency of electric motors," *IEEE Industry Applications Magazine*, vol. 17, no. 1, pp. 12–19, 2010.
- [27] C. U. Brunner, R. Werle, and R. Tieben, "The Motor Systems Retirement Program," 2015.
- [28] H. Gavrilă, V. Manescu, G. Paltanea, G. Scutaru, and I. Peter, "New Trends in Energy Efficient Electrical Machines," *Procedia Engineering*, vol. 181, pp. 568–574, 2017.
- [29] A. Marfoli, M. Di Nardo, M. Degano, C. Gerada, and W. Chen, "Rotor Design Optimization of Squirrel Cage Induction Motor-Part I: Problem Statement," *IEEE Transactions on Energy Conversion*, 2020.
- [30] M. Di Nardo, A. Marfoli, M. Degano, C. Gerada, and W. Chen, "Rotor Design Optimization of Squirrel Cage Induction Motor-Part II: Results Discussion," *IEEE Transactions on Energy Conversion*, 2020.
- [31] Z. Wang, Y. Enomoto, H. Tokoi, A. Komura, T. Obata, and K. Souma, "Development of IE5 high efficiency motor with iron-base amorphous magnetic cores," *Energy Efficiency in Motor Driven Systems (EEMODS)*, vol. 15, 2015.
- [32] P. Fanning, "IE5 and beyond," *Eureka*, 2020.
- [33] M. Božić, M. Rosić, B. Koprivica, M. Bjekić, and S. Antić, "Efficiency classes of three-phase, cage-induction motors (IE-code) software," in *INDEL2012, IX Symposium Industrial Electronics, INDEL*, 2012, pp. 87–91.
- [34] A. De Almeida, J. Fong, and H. Falkner, "New European ecodesign regulation proposal for electric motors and drives," in *Proceedings of the 9th International Conference on Energy Efficiency in Motor Driven Systems (EEMODS'15)*, 2015, pp. 15–17.
- [35] A. T. de Almeida, J. Fong, H. Falkner, and P. Bertoldi, "Policy options to promote energy efficient electric motors and drives in the EU," *Renewable and Sustainable Energy Reviews*, vol. 74, pp. 1275–1286, 2017.
- [36] J. Cui *et al.*, "Current progress and future challenges in rare-earth-free permanent magnets," *Acta Materialia*, vol. 158, pp. 118–137, 2018.
- [37] D. Bauer, D. Diamond, J. Li, D. Sandalow, T. Paul, and B. Wanner, "US Department of Energy Critical Materials Strategy," 2010.
- [38] "No Title," *USGS Mineral Commodities Summaries*.
- [39] "Magnetic Materials, a Global Strategic Business Report," *Analysts*, 2010.
- [40] J. Cui *et al.*, "Current progress and future challenges in rare-earth-free permanent magnets," *Acta Materialia*, vol. 158, pp. 118–137, 2018.
- [41] P. Nothnagel, K.-H. Müller, D. Eckert, and A. Handstein, "The influence of particle size on the coercivity of sintered NdFeB magnets," *Journal of magnetism and magnetic materials*, vol. 101, no. 1–3, pp. 379–381, 1991.
- [42] G. Bailey, N. Mancheri, and K. Van Acker, "Sustainability of permanent rare earth magnet motors in (H) EV industry," *Journal of Sustainable Metallurgy*, vol. 3, no. 3, pp. 611–626, 2017.
- [43] S. J. Chapman, *Electric machinery fundamentals*. McGraw-Hill, 2012.
- [44] Z. Zhong, S. Jiang, and G. Zhang, "Magnetic Equivalent Circuit Model of Interior Permanent-Magnet Synchronous Machine Considering Magnetic Saturation," *KINTEX Conference, Korea*, pp. 1–10, 2015.
- [45] J.-C. Urresty, J.-R. Riba, M. Delgado, and L. Romeral, "Detection of demagnetization faults in surface-mounted permanent magnet synchronous motors by means of the zero-sequence voltage component," *IEEE transactions on Energy conversion*, vol. 27, no. 1, pp. 42–51, 2012.
- [46] B. Z. Q. Zhu and D. Howe, "Electrical Machines and Drives for Electric, Hybrid, and Fuel Cell Vehicles," vol. 95, no. 4, 2007.
- [47] T. M. Jahns, "Flux-weakening regime operation of an interior permanent-magnet synchronous motor drive," *IEEE Transactions on Industry Applications*, no. 4, pp. 681–689, 1987.
- [48] T. M. Jahns, "Torque production in permanent-magnet synchronous motor drives with rectangular current excitation," *IEEE Transactions on Industry Applications*, no. 4, pp. 803–813, 1984.
- [49] T. Transi, M. Murataliyev, M. Degano, E. Preci, D. Gerada, and C. Gerada, "Influence of Rotor Design on Electromagnetic Performance in Interior Permanent Magnet Machines," in *IECON 2020 The 46th Annual Conference of the IEEE Industrial Electronics Society*, 2020, pp. 1021–1026. doi: 10.1109/IECON43393.2020.9255237.
- [50] M. Barcaro, N. Bianchi, and F. Magnussen, "Permanent-magnet optimization in permanent-magnet-assisted synchronous reluctance motor for a wide constant-power speed range," *IEEE Transactions on Industrial Electronics*, vol. 59, no. 6, pp. 2495–2502, 2011.
- [51] G. Pellegrino and F. Cupertino, "IPM motor rotor design by means of FEA-based multi-objective optimization," in *2010 IEEE International Symposium on Industrial Electronics*, 2010, pp. 1340–1346.
- [52] A. Vagati, G. Franceschini, I. Marongiu, and G. P. Troglia, "Design criteria of high performance synchronous reluctance motors," *Conference Record of the 1992 IEEE Industry Applications Society Annual Meeting*, pp. 66–73, 1992, doi: 10.1109/IAS.1992.244463.
- [53] B. Stumberger, G. Stumberger, D. Dolinar, A. Hamler, and M. Trlep, "Evaluation of Saturation and Cross-Magnetization Effects in Interior Permanent-Magnet," *Industry Applications, IEEE Transactions on*, vol. 39, no. 5, pp. 1264–1271, 2003.
- [54] P. Guglielmi, M. Pastorelli, and A. Vagati, "Impact of cross-saturation in sensorless control of transverse-laminated synchronous

- reluctance motors," *IEEE Transactions on Industrial Electronics*, vol. 53, no. 2, pp. 429–439, 2006.
- [55] E. Armando, R. I. Bojoi, P. Guglielmi, G. Pellegrino, and M. Pastorelli, "Experimental identification of the magnetic model of synchronous machines," *IEEE Transactions on Industry Applications*, vol. 49, no. 5, pp. 2116–2125, 2013.
- [56] S. Wang, M. Degano, J. Kang, A. Galassini, and C. Gerada, "A novel Newton-Raphson-based searching method for the MTPA control of PMSynRM considering magnetic and cross saturation," in *2018 XIII International Conference on Electrical Machines (ICEM)*, 2018, pp. 1360–1366.
- [57] A. Vagati, "The synchronous reluctance solution: a new alternative in AC drives," in *Proceedings of IECON'94-20th Annual Conference of IEEE Industrial Electronics*, 1994, vol. 1, pp. 1–13.
- [58] A. Vagati, G. Franceschini, I. Marongiu, and G. P. Troglia, "Design criteria of high performance synchronous reluctance motors," in *Conference Record of the 1992 IEEE Industry Applications Society Annual Meeting*, 1992, pp. 66–73.
- [59] A. Fratta, G. P. Troglia, A. Vagati, and F. Villata, "Evaluation of torque ripple in high performance synchronous reluctance machines," in *Conference Record of the 1993 IEEE Industry Applications Conference Twenty-Eighth IAS Annual Meeting*, 1993, pp. 163–170.
- [60] A. Vagati, M. Pastorelli, G. Franceschini, and S. C. Petrace, "Design of low-torque-ripple synchronous reluctance motors," *IEEE Transactions on industry applications*, vol. 34, no. 4, pp. 758–765, 1998.
- [61] T. A. Lipo, T. J. E. Miller, A. Vagati, I. Boldea, L. Malesani, and T. Fukao, "Synchronous reluctance drives," in *Conf. Rec. IEEE IAS Annu. Meeting*, 1994, vol. 10.
- [62] E. Armando, P. Guglielmi, G. Pellegrino, M. Pastorelli, and A. Vagati, "Accurate modeling and performance analysis of IPM-PMASR motors," *IEEE Transactions on Industry Applications*, vol. 45, no. 1, pp. 123–130, 2009.
- [63] N. Bianchi, "Synchronous reluctance and interior permanent magnet motors," *Electrical Machines Design Control and Diagnosis (WEMDCD)*, *2013 IEEE Workshop on*, vol. 3, pp. 75–84, 2013, doi: 10.1109/WEMDCD.2013.6525167.
- [64] M. Gamba, G. Pellegrino, and F. Cupertino, "Optimal number of rotor parameters for the automatic design of Synchronous Reluctance machines," *Proceedings - 2014 International Conference on Electrical Machines, ICEM 2014*, pp. 1334–1340, 2014, doi: 10.1109/ICELMACH.2014.6960355.
- [65] M. Degano, E. Carraro, and N. Bianchi, "Selection criteria and robust optimization of a traction PM-assisted synchronous reluctance motor," *IEEE Transactions on Industry Applications*, vol. 51, no. 6, pp. 4383–4391, 2015.
- [66] R. R. Moghaddam, F. Magnussen, and C. Sadarangani, "Theoretical and experimental reevaluation of synchronous reluctance machine," *IEEE Transactions on Industrial Electronics*, vol. 57, no. 1, pp. 6–13, 2009.
- [67] G. Pellegrino, A. Vagati, P. Guglielmi, and B. Boazzo, "Performance comparison between surface-mounted and interior PM motor drives for electric vehicle application," *IEEE Transactions on Industrial Electronics*, vol. 59, no. 2, pp. 803–811, 2011.
- [68] T. J. E. Miller, A. Hutton, C. Cossar, and D. A. Staton, "Design of a synchronous reluctance motor drive," *IEEE Transactions on industry applications*, vol. 27, no. 4, pp. 741–749, 1991.
- [69] T. Matsuo and T. A. Lipo, "Rotor design optimization of synchronous reluctance machine," *IEEE Transactions on Energy Conversion*, vol. 9, no. 2, pp. 359–365, 1994.
- [70] D. A. Staton, T. J. E. Miller, and S. E. Wood, "Maximising the saliency ratio of the synchronous reluctance motor," *IEE Proceedings B Electric Power Applications*, vol. 140, no. 4, p. 249, 1993, doi: 10.1049/ip-b.1993.0031.
- [71] I. Boldea, Z. X. Fu, and S. A. Nasar, "Performance evaluation of axially-laminated anisotropic (ALA) rotor reluctance synchronous motors," in *Conference Record of the 1992 IEEE Industry Applications Society Annual Meeting*, pp. 212–218. doi: 10.1109/IAS.1992.244292.
- [72] M. Degano, H. Mahmoud, N. Bianchi, and C. Gerada, "Synchronous reluctance machine analytical model optimization and validation through finite element analysis," *2016 XXII International Conference on Electrical Machines (ICEM)*, pp. 585–591, 2016, doi: 10.1109/ICELMACH.2016.7732585.
- [73] B. J. Chalmers and L. Musaba, "Design and field-weakening performance of a synchronous reluctance motor with axially laminated rotor," *IEEE Transactions on Industry Applications*, vol. 34, no. 5, pp. 1035–1041, 1998.
- [74] M. J. Kamper, F. S. der Merwe, and S. Williamson, "Direct finite element design optimisation of the cageless reluctance synchronous machine," *IEEE Transactions on Energy Conversion*, vol. 11, no. 3, pp. 547–555, 1996.
- [75] E. C. F. Lovelace, "Optimization of a magnetically saturable interior permanent-magnet synchronous machine drive," Massachusetts Institute of Technology, 2000.
- [76] S. Talebi, P. Niazi, and H. A. Toliyat, "Design of permanent magnet-assisted synchronous reluctance motors made easy," in *2007 IEEE Industry Applications Annual Meeting*, 2007, pp. 2242–2248.
- [77] R. R. Moghaddam and F. Gyllensten, "Novel high-performance SynRM design method: An easy approach for a complicated rotor topology," *IEEE Transactions on Industrial Electronics*, vol. 61, no. 9, pp. 5058–5065, 2014, doi: 10.1109/TIE.2013.2271601.
- [78] M. J. Kamper and A. F. Volsdhenk, "Effect of rotor dimensions and cross magnetisation on Ld and Lq inductances of reluctance synchronous machine with cageless flux barrier rotor," *IEE Proceedings-Electric Power Applications*, vol. 141, no. 4, pp. 213–220, 1994.
- [79] F. Cupertino, G. M. Pellegrino, E. Armando, and C. Gerada, "A SyR and IPM machine design methodology assisted by optimization algorithms," in *2012 IEEE Energy Conversion Congress and Exposition (ECCE)*, 2012, pp. 3686–3691.
- [80] H. Mahmoud, M. Degano, G. Bacco, N. Bianchi, and C. Gerada, "Synchronous Reluctance Motor Iron Losses: Analytical Model and Optimization," *2018 IEEE Energy Conversion Congress and Exposition, ECCE 2018*, pp. 1640–1647, 2018, doi: 10.1109/ECCE.2018.8558292.
- [81] G. Pellegrino, F. Cupertino, and C. Gerada, "Automatic Design of Synchronous Reluctance Motors Focusing on Barrier Shape Optimization," *IEEE Transactions on Industry Applications*, vol. 51, no. 2, pp. 1465–1474, 2015, doi: 10.1109/TIA.2014.2345953.
- [82] G. R. Slemon, "On the Design of High-Performance Surface-Mounted PM Motors," *IEEE Transactions on Industry Applications*, vol. 30, no. 1, pp. 134–140, 1993, doi: 10.1109/28.273631.
- [83] M. Galea, C. Gerada, T. Raminosa, and P. Wheeler, "A Thermal Improvement Technique for the Phase Windings of Electrical Machines," vol. 48, no. 1, pp. 79–87, 2012.
- [84] C. Sciascera, P. Giangrande, L. Papini, C. Gerada, and M. Galea, "Analytical thermal model for fast stator winding temperature prediction," *IEEE Transactions on Industrial Electronics*, vol. 64, no. 8, pp. 6116–6126, 2017.
- [85] M. Murataliyev, M. Degano, and M. Galea, "A Novel Sizing Approach for Synchronous Reluctance Machines," *IEEE Transactions on Industrial Electronics*, vol. 0046, no. 2, 2020, doi: 10.1109/TIE.2020.2975461.
- [86] M. Murataliyev et al., "Homothetic Design in Synchronous Reluctance Machines and Effects on Torque Ripple," *IEEE Transactions on Energy Conversion*, p. 1, 2020, doi: 10.1109/TEC.2020.3042441.
- [87] N. Bianchi, S. Bolognani, D. Bon, and M. Dai Pre, "Rotor flux-barrier design for torque ripple reduction in synchronous reluctance and PM-assisted synchronous reluctance motors," *IEEE Transactions on Industry Applications*, vol. 45, no. 3, pp. 921–928, 2009.
- [88] F. Cupertino, G. Pellegrino, and C. Gerada, "Design of synchronous reluctance motors with multiobjective optimization algorithms," *IEEE Transactions on Industry Applications*, vol. 50, no. 6, pp. 3617–3627, 2014.
- [89] N. Bianchi, M. Degano, and E. Fornasiero, "Sensitivity analysis of torque ripple reduction of synchronous reluctance and interior PM motors," *IEEE Transactions on Industry Applications*, vol. 51, no. 1, pp. 187–195, 2014.
- [90] M. Degano, E. Carraro, and N. Bianchi, "Selection Criteria and Robust Optimization of a Traction PM Assisted Synchronous

- Reluctance Motor,” vol. 9994, no. c, 2015, doi: 10.1109/TIA.2015.2443091.
- [91] N. Bianchi, S. Bolognani, D. Bon, and M. D. Prè, “Rotor flux-barrier design for torque ripple reduction in synchronous reluctance and PM-assisted synchronous reluctance motors,” *IEEE Transactions on Industry Applications*, vol. 45, no. 3, pp. 921–928, 2009, doi: 10.1109/TIA.2009.2018960.
- [92] M. Murataliyev *et al.*, “Homothetic Design in Synchronous Reluctance Machines and Effects on Torque Ripple,” *IEEE Transactions on Energy Conversion*, p. 1, 2020, doi: 10.1109/TEC.2020.3042441.
- [93] M. Murataliyev *et al.*, “A Homothetic Scaling Criteria for Synchronous Reluctance Machines Design,” *IEEE TRANSACTION ON ENERGY CONVERSION*.
- [94] H. Hofmann and S. R. Sanders, “High-speed synchronous reluctance machine with minimized rotor losses,” *IEEE Transactions on Industry Applications*, vol. 36, no. 2, pp. 531–539, 2000.
- [95] C. Babetto, G. Bacco, and N. Bianchi, “Synchronous Reluctance Machine Optimization for High Speed Applications,” *IEEE Transactions on Energy Conversion*, vol. 8969, no. c, pp. 1–8, 2018, doi: 10.1109/TEC.2018.2800536.
- [96] M. Di Nardo, G. Lo Calzo, M. Galea, and C. Gerada, “Design optimization of a high-speed synchronous reluctance machine,” *IEEE Transactions on Industry Applications*, vol. 54, no. 1, pp. 233–243, 2017.
- [97] C. Babetto, G. Bacco, and N. Bianchi, “Design methodology for high-speed synchronous reluctance machines,” *IET Electric Power Applications*, vol. 12, no. 8, pp. 1110–1116, 2018.
- [98] O. Payza, Y. Demir, and M. Aydin, “Investigation of Losses for a Concentrated Winding High-Speed Permanent Magnet-Assisted Synchronous Reluctance Motor for Washing Machine Application,” *IEEE Transactions on Magnetics*, vol. 54, no. 11, pp. 1–5, 2018.
- [99] G. Gallicchio *et al.*, “High Speed Synchronous Reluctance Machines: Modeling, Design and Limits,” *IEEE Transactions on Energy Conversion*, 2021.
- [100] M. di Nardo *et al.*, “High Speed Synchronous Reluctance Machines: Materials Selection and Performance Boundaries,” *IEEE Transactions on Transportation Electrification*, 2021.
- [101] T. A. Lipo, “Synchronous reluctance machines—a viable alternative for ac drives?,” *Electric Machines and Power Systems*, vol. 19, no. 6, pp. 659–671, 1991.
- [102] A. Vagati, A. Canova, M. Chiampi, M. Pastorelli, and M. Repetto, “Design refinement of synchronous reluctance motors through finite-element analysis,” *IEEE Transactions on Industry Applications*, vol. 36, no. 4, pp. 1094–1102, 2000, doi: 10.1109/28.855965.
- [103] H. D. Do, A. Anuchin, D. Shpak, A. Zharkov, and A. Rusakov, “Overvoltage protection for interior permanent magnet synchronous motor testbench,” in *2018 25th International Workshop on Electric Drives: Optimization in Control of Electric Drives (IWED)*, 2018, pp. 1–4. doi: 10.1109/IWED.2018.8321396.
- [104] M. J. Kamper, “Reluctance Synchronous Machine Drives – a Viable Alternative?,” *IEEE Joint IAS/PELS/IES Chapter Meeting. Graz (Austria)*, no. July, 2013.
- [105] H. Murakami, Y. Honda, H. Kiriya, S. Morimoto, and Y. Takeda, “The performance comparison of SPMSM, IPMSM and SynRM in use as air-conditioning compressor,” in *Conference Record of the 1999 IEEE Industry Applications Conference. Thirty-Forth IAS Annual Meeting (Cat. No.99CH36370)*, vol. 2, pp. 840–845. doi: 10.1109/IAS.1999.801607.
- [106] M. D. Nardo, G. L. Calzo, M. Galea, and C. Gerada, “Design Optimization of a High-Speed Synchronous Reluctance Machine,” *IEEE Transactions on Industry Applications*, vol. 54, no. 1, pp. 233–243, 2018, doi: 10.1109/TIA.2017.2758759.
- [107] M. Degano *et al.*, “Optimised Design of Permanent Magnet Assisted Synchronous Reluctance Machines for Household Appliances,” *IEEE Transactions on Energy Conversion*, p. 1, 2021, doi: 10.1109/TEC.2021.3076675.
- [108] C. R. N.-O. E. Steel, “Sheet and Strip Delivered in the Fully Processed State,” *SIST Standard EN*, vol. 10106, p. 2014, 2014.
- [109] H.-C. Liu and J. Lee, “Optimum Design of an IE4 Line-Start Synchronous Reluctance Motor Considering Manufacturing Process Loss Effect,” *IEEE Transactions on Industrial Electronics*, vol. 65, no. 4, pp. 3104–3114, 2018, doi: 10.1109/TIE.2017.2758738.
- [110] M. Gamba, E. Armando, G. Pellegrino, A. Vagati, B. Janjic, and J. Schaab, “Line-start synchronous reluctance motors: Design guidelines and testing via active inertia emulation,” in *2015 IEEE Energy Conversion Congress and Exposition (ECCE)*, 2015, pp. 4820–4827. doi: 10.1109/ECCE.2015.7310340.
- [111] M. Gamba, G. Pellegrino, A. Vagati, and F. Villata, “Design of a line-start synchronous reluctance motor,” in *2013 International Electric Machines Drives Conference*, 2013, pp. 648–655. doi: 10.1109/IEMDC.2013.6556163.
- [112] A. Castagnini, T. Käsäkangas, J. Kolehmainen, and P. S. Termini, “Analysis of the starting transient of a synchronous reluctance motor for direct-on-line applications,” in *2015 IEEE International Electric Machines Drives Conference (IEMDC)*, 2015, pp. 121–126. doi: 10.1109/IEMDC.2015.7409047.
- [113] ABB, “Synchronous reluctance motor-drive package for machine builders: High performance for ultimate machine design,” 2014.
- [114] “REEL SuPremE® motor: Premium IE5/IE4 efficiency without magnets.” [Online]. Available: https://www.ksb.com/REEL-en/products-solutions/Synchronous_reluctance_motors/reel-supreme-ie5/
- [115] “Driving fluid flow engines towards the ultimate productivity.” [Online]. Available: <https://new.siemens.com/global/en/products/drives/topic-areas/reluctance-drive-system.html>



Mukhammed Murataliyev (Member, IEEE) received his Masters degree in electrical engineering from the University of Nottingham, Malaysia in 2016. He received a Ph.D degree from University of Nottingham China and UK in 2021, with a focus on novel synchronous reluctance motor design and optimization methods. From 2018 – 2020 he was a Researcher with the Key Laboratory of More Electric Aircraft Technology of Zhejiang Province. Since 2021, he joined the Power Electronics and Machine Control Group of the University of Nottingham, UK as a Research Fellow. He was a member of several projects related to the design of electrical machines for traction, aerospace, and industrial applications. His main research interest includes design and modeling of reluctance and permanent magnet machines for industrial and aerospace applications.



Michele Degano (Senior Member, IEEE) received the Master’s degree in electrical engineering from the University of Trieste, Italy, in 2011, and the Ph.D. degree in industrial engineering from the University of Padova, Italy, in 2015. Between 2014 and 2016, he was a Postdoctoral Researcher at The University of Nottingham, U.K., where he joined the Power Electronics, Machines and Control (PEMC) Research Group. In 2016 he was appointed Assistant Professor in Advanced Electrical Machines, at The University of Nottingham, U.K. He was promoted Associate Professor in 2020. His main research focuses on electrical machines and drives for industrial, automotive, railway and aerospace applications, ranging from small to large power. He is currently the PEMC Director of Industrial Liaison leading research projects for the development of future hybrid electric aerospace platforms and electric transports.



Mauro Di Nardo (Member, IEEE) received the M.Sc. (Hons.) degree in electrical engineering from the Polytechnic University of Bari, Italy, in 2012, and the Ph.D. degree in electrical machine design from the University of Nottingham, U.K., in 2017. From 2017 to 2019, he was Head of the AROL research team within the Polytechnic University of Bari leading industrial R&D projects on electrical

drives design for mechatronics applications. Since the 2019, he joined the Power Electronics and Machine Control Group of the University of Nottingham as Research Fellow. His research interests include the analysis, modeling, and optimizations of electrical machines, including permanent magnet and synchronous reluctance topologies for automotive and aerospace sectors as well as induction motor for industrial applications.



Nicola Bianchi (Fellow, IEEE), received the M.Sc. and Ph.D. degrees in electrical engineering from the University of Padova, Padova, Italy, in 1991 and 1995, respectively. In 1998, he joined the Department of Electrical Engineering, University of Padova, as an Assistant Professor, where since 2005, he has been an Associate Professor in Electrical Machines, Converters, and Drives with the

Electric Drive Laboratory, Department of Electrical Engineering. He has authored and coauthored several scientific papers and international books on electrical machines and drives. His research interests include the field of design of electrical machines, particularly for drive applications. Dr. Bianchi was the recipient of five awards for best conference and journal papers. He is a member of the Electric Machines Committee and the Electrical Drives Committee of the IEEE Industry Applications Society. He was a Technical Program Chair for the IEEE Energy Conversion Congress and Exposition in 2014 and is currently an Associate Editor for the IEEE TRANSACTIONS ON INDUSTRY APPLICATIONS.



Chris Gerada (Senior Member, IEEE) is an Associate Pro-ViceChancellor for Industrial Strategy and Impact and Professor of Electrical Machines. His principal research interest lies in electromagnetic energy conversion in electrical machines and drives, focusing mainly on transport electrification. He has secured over £20M of funding through major industrial, European and UK grants and authored more

than 350 referred publications. He received the Ph.D. degree in numerical modelling of electrical machines from The University of Nottingham, Nottingham, U.K., in 2005. He subsequently worked as a Researcher with The University of Nottingham on high-performance electrical drives and on the design and modelling of electromagnetic actuators for aerospace applications. In 2008, he was appointed as a Lecturer in electrical machines; in 2011, as an Associate Professor; and in 2013, as a Professor at The University of Nottingham. He was awarded a Research Chair from the Royal Academy of Engineering in 2013. Prof. Gerada served as an Associate Editor for the IEEE Transactions on Industry Applications and is the past Chair of the IEEE IES Electrical Machines Committee.